# Structure of hepatitis C virus envelope glycoprotein E2 antigenic site 412-423 in complex with antibody AP33

**Running title:** Structure of HCV E2 antigenic site 412-423

Leopold Kong[a], Erick Giang[b], Travis Nieusma[a], Justin B. Robbins[b], Marc C. Deller[a,d], Robyn L. Stanfield[a], Ian A. Wilson[a,c,d,1], and Mansun Law[b,1]

Departments of [a]Molecular Biology and [b]Immunology and Microbial Science, and [c]The Skaggs Institute for Chemical Biology, The Scripps Research Institute, La Jolla, CA 92037. [d]Joint Center for Structural Genomics, http://www.jcsg.org, USA.

[1]To whom correspondence may be addressed. E-mail: wilson@scripps.edu or mlaw@scripps.edu

Data deposition: The atomic coordinates have been deposited in the Protein Data Bank, www.pdb.org (PBD ID code 4G6A).

## SUPPLEMENTAL MATERIALS

### Supplemental materials and methods.

#### Antibody production

The $V_H$ and $V_L$ domains of antibody AP33 were fused with human $C_H$1-3 and $C_L$ as a murine-human chimeric antibody using the pIgG1 vector for high-level protein expression (10). This chimeric antibody is referred as MAb huAP33 here to distinguish it from the original mouse MAb discovered by Patel and co-workers (16). The chimeric antibody bound E1E2, and the binding could be inhibited using linear peptides encoding the proposed antigenic site (Fig. S1). The MAb also neutralized HCV as expected (Fig. S1). To prepare the Fab fragment for crystallization studies, $C_H$2-3 domains in the expression vector were deleted and soluble Fab was produced by transient transfection of 293F cells with the recombinant DNA. The Fab was purified by affinity chromatography using a rabbit anti-human Fab antibody column followed by passage through a monoS 10/100 GL cation exchange column (GE Healthcare). The primary peak was then further purified using size exclusion chromatography with a Superdex 200 (GE Healthcare) column.

#### Complex formation and crystallization using iterative micro-batch seeding

The AP33 Fab was concentrated to 8-12 mg/mL using an Amicon centrifugal ultrafiltration unit (Millipore) with a 10 kDa molecular weight cutoff. The concentrated Fab and the R12 peptide encoding the antigenic site (9) were incubated at a 1:10 molar ratio overnight at 4$^{o}$C in 150 mM NaCl, 20 mM Tris-HCl pH 7.2 to form the complex. Samples were screened for crystallization using the 384 conditions of the JCSG Core Suite (Qiagen) at both 277 and 293 K using the JCSG robotic Crystalmation system (Rigaku). Crystallization was performed using the nanodroplet vapor diffusion method (17) with standard JCSG crystallization protocols (11). Sitting drops composed of 200 nl of protein sample were mixed with 200 nl of crystallization reagent in a sitting drop format and were equilibrated against a 50 µl reservoir of crystallization reagent. After approximately 3 days at 20$^{o}$C, thin bundles of needle-shaped crystals formed in 17% (w/v) PEG 4000, 8.5% (v/v) 2-propanol, 15% (v/v) glycerol and 0.085 M Sodium HEPES, pH 7.5 (JCSG Core Suite 2, well B11). These initial crystals were too small for diffraction studies and were crushed in a Seed Bead tube (Hampton Research) for use in micro-batch seeding (5, 8). The crystals were placed into the Seed Bead tube containing 50 µl of mother liquor and then vortexed for 3 x 30 s, keeping the tube on ice between manipulations. Micro-batch seeding was carried out using sitting drops composed of 150 nl of protein, 100 nl of crystallization reagent and 50 nl of seed stock as implemented by an Oryx 8

robot (Douglas Instruments) and plates were incubated at 16$^{o}$C. The crystallization reagent used in this first round of seeding consisted of a custom optimization screen centered on the initial crystallization hit with varying PEG4000 (5–27%, w/v) and 2-propanol (0.5–14.5%, v/v) concentration. Custom screens were formulated by an Alchemist robotic system (Rigaku). The first round of micro-batch seeding resulted in thin plate crystals that were unsuitable for diffraction studies. These plates were submitted to a further round of micro-batch seeding and improved hexagonal plates of diffraction quality were finally achieved in the same condition.

**Data collection**

The optimized, hexagonal crystals diffracted to 2.5Å at beamline 11-1 of the Stanford Synchrotron Radiation Lightsource (SSRL). Data were collected at 100 K to a completeness of 91% with an overall $R_{sym}$ of 10% (23% in the high resolution shell) (Table S1). Data were indexed, processed and scaled with HKL-2000 (15) in the monoclinic space group $P2_1$ with unit cell parameters $a$ = 44.9Å, $b$ = 191.8Å, $c$ = 59.4Å, $\beta$= 111.1˚.

**Structure Refinement**

The structure was determined by the molecular replacement method using Phaser (13) with the HCV1 Fab structure (PDB ID: 4DGV) as an initial model. Model building was carried out using Coot-0.6.2 (6) and refinement was implemented with Phenix (1). Final $R_{cryst}$ and $R_{free}$ values are 17.8 % and 21.9 %, respectively. Buried molecular surface areas were analyzed with MS (4) using a 1.7 Å probe radius and standard van der Waals radii, and van der Waals contacts and hydrogen bonds were evaluated with CONTACSYM (18, 19) and HBPLUS (14). Surface potential and electrostatics were calculated using APBS (2) and all structural visualizations were generated with PyMOL (The PyMOL Molecular Graphics System, Version 1.2r3pre, Schrödinger, LLC.). For the Fab, the residues were renumbered according to the Kabat scheme (12).

## SUPPLEMENTAL FIGURE

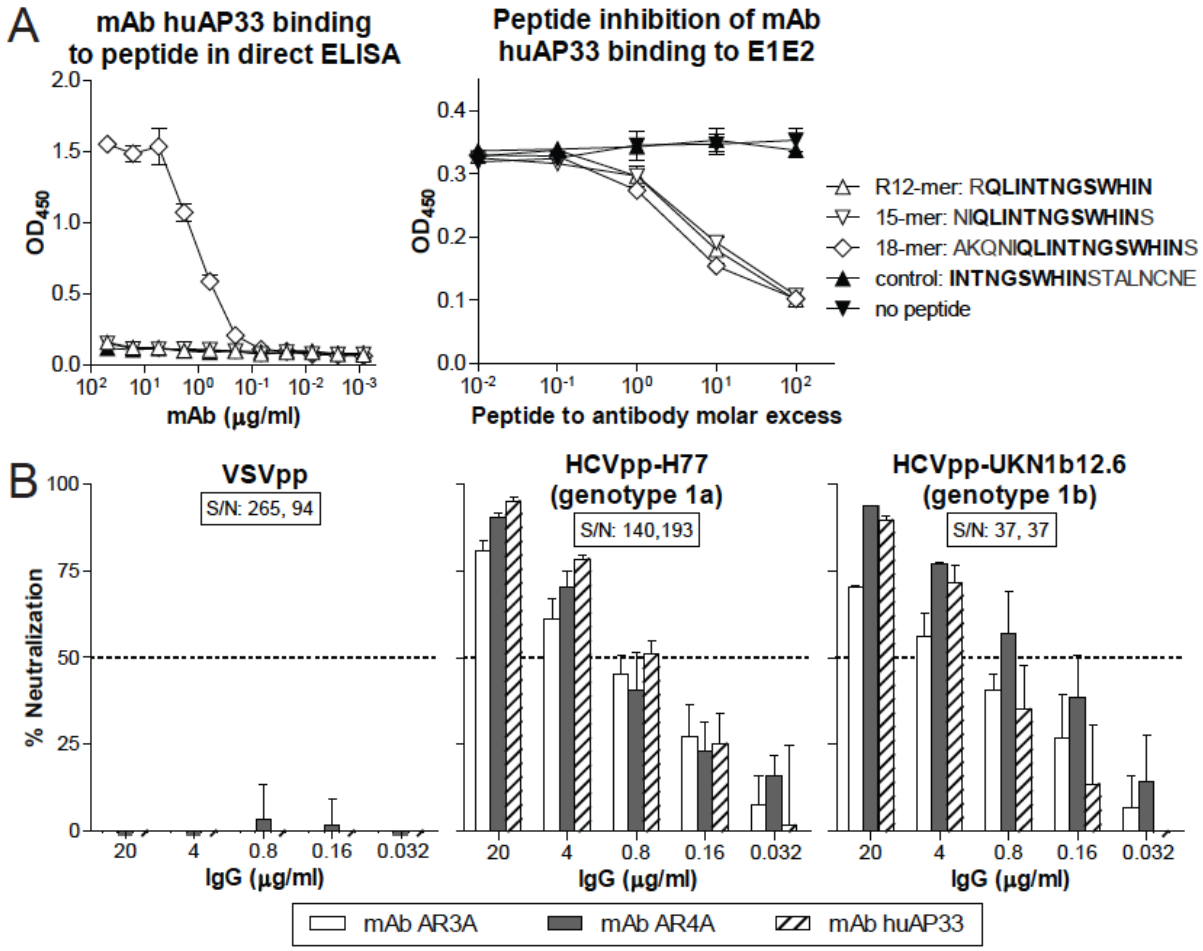


**FIG. S1**. Biological activities of recombinant mouse-human chimeric antibody AP33 (MAb huAP33). (A) Peptide candidates for crystallography. The binding of MAb huAP33 to three candidate peptides (R12-mer, 15-mer and 18-mer) was first evaluated by direct ELISA (left panel). The MAb only binds the 18-mer when the peptides were coated directly onto microwells. However, in solution, all 3 peptides blocked antibody binding to E1E2 at similar levels (right panel). The epitope sequence is in bold and the control peptide with truncated epitope sequence did not block MAb binding. The soluble R12-mer was used in crystallization experiments. (B) Neutralization of HCV by MAb huAP33. The chimeric MAb neutralized HCV pseudotype virus particles (HCVpp) displaying the genotype 1a or 1b E1E2, but not the control envelope glycoprotein G from vesicular stomatitis virus (VSVpp). The mAbs AR3A and AR4A are control neutralizing mAbs to E2 and the E1E2 complex, respectively (7).

**Table S1.** Data Collection and Refinement Statistics for Fab AP33

| Data collection | AP33 Fab |
|---|---|
| Beamline | SSRL11-1 |
| Wavelength (Å) | 0.98000 |
| Space group | $P2_1$ |
| Unit cell parameters | a = 44.9<br>b = 191.8<br>c = 59.4 Å<br>β = 111.1° |
| Resolution (Å) | 47.97-2.50<br>(2.54-2.50)[a] |
| Observations | 188,654 |
| Unique reflections | 29,450 (966) [a] |
| Redundancy | 6.4 (4.4) [a] |
| Completeness (%) | 91.3 (61.3) [a] |
| $\langle I/\sigma_I \rangle$ | 16.0 (5.7) [a] |
| $R_{sym}$ [b] | 0.10 (0.23) [a, b] |
| **Refinement statistics** | |
| Resolution (Å) | 47.97-2.50<br>(2.58-2.50) |
| Reflections (work) | 27,907 (1718) |
| Reflections (test) | 1,502 (89) |
| $R_{cryst}$ (%)[c] | 17.8[c] (23.3) |
| $R_{free}$ (%)[d] | 22.0[d] (32.0) |
| Average B-value (Å$^2$) | 34.1 |
| Wilson B-value (Å$^2$) | 32.5 |
| **RMSD from ideal geometry** | |
| Bond length (Å) | 0.003 |
| Bond angles (°) | 0.79 |
| **Ramachandran statistics (%)[e]** | |
| Favored | 97.3 |
| Outliers | 0.7 |
| PDB ID | 4G6A |

[a] Numbers in parentheses refer to the highest resolution shell.

[b] $R_{sym} = \Sigma_{hkl}\Sigma_i \mid I_{hkl,i} - \langle I_{hkl} \rangle \mid / \Sigma_{hkl}\Sigma_i I_{hkl,I}$, where $I_{hkl,i}$ is the scaled intensity of the $i^{th}$ measurement of relection h, k, l, $\langle I_{hkl} \rangle$ is the average intensity for that reflection, and $n$ is the redundancy (20).

[c] $R_{cryst} = \Sigma_{hkl} \mid F_o - F_c \mid / \Sigma_{hkl} \mid F_o \mid \times 100$

[d] $R_{free}$ was calculated as for $R_{cryst}$, but on a test set comprising 5% of the data excluded from refinement.

[e] These values were calculated using Molprobity (3).

**Table S2.** Van der Waals interactions between E2 peptide and AP33 Fab 1[a]

| Fab Residue | Atom[b] | Peptide Residue | Atom[b] | Distance (Å) |
|---|---|---|---|---|
| $TYR^{H33}$ | Cδ2 | TRP420 | Cη2 | 3.9 |
| $TYR^{H33}$ | Cε1 | ASN415 | Cβ | 3.8 |
| $TYR^{H33}$ | Cε2 | TRP420 | Cη2 | 3.6 |
| $TYR^{H33}$ | Cε2 | TRP420 | Cζ3 | 3.8 |
| $TYR^{H33}$ | Cζ | ASN415 | N | 3.7 |
| $TYR^{H33}$ | Cζ | ASN415 | Cβ | 3.8 |
| $TYR^{H33}$ | Cζ | TRP420 | Cη2 | 4.1 |
| $TYR^{H33}$ | Oη | ILE414 | Cα | 3.5 |
| $TYR^{H33}$ | Oη | ILE414 | C | 3.6 |
| $TYR^{H33}$ | Oη | ASN415 | Cα | 3.6 |
| $TYR^{H33}$ | Oη | ASN415 | Cβ | 3.7 |
| $TYR^{H33}$ | Oη | ILE414 | Cβ | 3.8 |
| $TYR^{H50}$ | Cε1 | ASN415 | Oδ1 | 3.5 |
| $TYR^{H50}$ | Cζ | ASN415 | Oδ1 | 3.3 |
| $TYR^{H50}$ | Oη | ASN415 | Oδ1 | 2.3 |
| $TYR^{H50}$ | Oη | ASN415 | Cγ | 3.3 |
| $TYR^{H50}$ | Oη | ASN415 | O | 3.5 |
| $TYR^{H50}$ | Oη | ASN415 | Cβ | 3.7 |
| $TYR^{H50}$ | Oη | ASN415 | C | 3.8 |
| $TYR^{H58}$ | Cδ2 | ASN417 | C | 3.7 |
| $TYR^{H58}$ | Cδ2 | GLY418 | N | 3.8 |
| $TYR^{H58}$ | Cδ2 | ASN417 | Cα | 3.9 |
| $TYR^{H58}$ | Cε1 | GLY418 | Cα | 3.9 |
| $TYR^{H58}$ | Cε2 | ASN417 | O | 3.6 |
| $TYR^{H58}$ | Cε2 | ASN417 | C | 3.6 |
| $TYR^{H58}$ | Cε2 | GLY418 | N | 3.8 |
| $TYR^{H58}$ | Cε2 | GLY418 | Cα | 3.9 |
| $TYR^{H58}$ | Cζ | GLY418 | Cα | 3.7 |
| $TYR^{H58}$ | Oη | GLY418 | Cα | 4.0 |
| $ILE^{H95}$ | Cγ2 | TRP420 | Cζ2 | 4.2 |
| $ILE^{H95}$ | Cγ2 | TRP420 | Cη2 | 4.2 |
| $TYR^{H100}$ | Cδ1 | TRP420 | Cζ3 | 3.4 |
| $TYR^{H100}$ | Cδ1 | TRP420 | Cε3 | 3.7 |
| $TYR^{H100}$ | Cδ1 | TRP420 | Cη2 | 3.8 |
| $TYR^{H100}$ | Cε1 | LEU413 | Cβ | 3.5 |
| $TYR^{H100}$ | Cε1 | TRP420 | Cζ3 | 3.6 |
| $TYR^{H100}$ | Cε1 | LEU413 | O | 3.7 |
| $TYR^{H100}$ | Cε1 | TRP420 | Cε3 | 3.8 |
| $TYR^{H100}$ | Cε1 | LEU413 | Cα | 4.1 |
| $TYR^{H100}$ | Cε1 | LEU413 | Cδ1 | 4.1 |
| $TYR^{H100}$ | Cζ | LEU413 | N | 3.8 |
| $TYR^{H100}$ | Cζ | LEU413 | Cβ | 3.8 |
| $TYR^{H100}$ | Cζ | LEU413 | Cδ1 | 4.1 |
| $TYR^{H100}$ | Oη | GLN412 | C | 3.5 |
| $TYR^{H100}$ | Oη | GLN412 | Cα | 3.5 |

| | | | | |
|---|---|---|---|---|
| $TYR^{H100}$ | Oη | LEU413 | Cβ | 3.6 |
| $TYR^{H100}$ | Oη | LEU413 | Cα | 3.7 |
| $TYR^{H100}$ | Oη | LEU413 | Cγ | 3.9 |
| $TYR^{L28}$ | Cβ | LEU413 | Cδ2 | 4.3 |
| $TYR^{L28}$ | Cγ | LEU413 | Cδ2 | 4.0 |
| $TYR^{L28}$ | Cδ1 | ILE422 | Cγ2 | 3.8 |
| $TYR^{L28}$ | Cδ2 | LEU413 | Cδ2 | 4.2 |
| $TYR^{L28}$ | Cε1 | ILE422 | Cγ2 | 3.8 |
| $TYR^{L28}$ | Cε1 | ILE422 | Cγ1 | 3.8 |
| $TYR^{L28}$ | Cε1 | ILE422 | N | 3.9 |
| $TYR^{L28}$ | Cε1 | ILE422 | Cδ1 | 4.1 |
| $TYR^{L28}$ | Cε2 | HIS421 | Cα | 3.5 |
| $TYR^{L28}$ | Cε2 | TRP420 | O | 3.5 |
| $TYR^{L28}$ | Cε2 | HIS421 | Cβ | 3.8 |
| $TYR^{L28}$ | Cζ | HIS421 | Cα | 3.6 |
| $TYR^{L28}$ | Cζ | HIS421 | Cβ | 3.7 |
| $TYR^{L28}$ | Cζ | ILE422 | N | 3.8 |
| $TYR^{L28}$ | Oη | HIS421 | Cβ | 3.1 |
| $TYR^{L28}$ | Oη | HIS421 | Cα | 3.6 |
| $PHE^{L32}$ | Cδ1 | TRP420 | Cδ1 | 4.2 |
| $PHE^{L32}$ | Cε1 | TRP420 | Cδ1 | 4.0 |
| $PHE^{L32}$ | Cε1 | TRP420 | Cγ | 4.0 |
| $PHE^{L32}$ | Cε1 | LEU413 | Cδ1 | 4.2 |
| $PHE^{L32}$ | Cζ | LEU413 | Cδ1 | 3.6 |
| $PHE^{L32}$ | Cζ | TRP420 | Cβ | 3.8 |
| $PHE^{L32}$ | Cζ | TRP420 | Cγ | 4.1 |
| $ASN^{L91}$ | O | TRP420 | Cδ1 | 3.1 |
| $ASN^{L92}$ | Cα | GLY418 | O | 3.3 |
| $ASN^{L92}$ | C | GLY418 | O | 3.3 |
| $ASN^{L92}$ | O | GLY418 | O | 3.5 |
| $ASN^{L92}$ | O | SER419 | Oγ | 3.6 |
| $ASN^{L92}$ | O | SER419 | Cα | 3.7 |
| $ASN^{L92}$ | Oδ1 | TRP420 | Cδ1 | 3.4 |
| $ASN^{L92}$ | Oδ1 | TRP420 | Cβ | 3.5 |
| $ASN^{L92}$ | Oδ1 | TRP420 | Cα | 3.8 |
| $TRP^{L96}$ | Cε2 | GLY418 | O | 3.8 |
| $TRP^{L96}$ | Nε1 | GLY418 | Cα | 3.6 |
| $TRP^{L96}$ | Nε1 | GLY418 | C | 3.7 |
| $TRP^{L96}$ | Cζ2 | ASN415 | Nδ2 | 3.7 |
| $TRP^{L96}$ | Cζ2 | GLY418 | O | 3.9 |

[a] Interactions determined by CONTACSYM (18, 19). Numbering for the peptide follows the HCV E2 numbering scheme. Fab numbering follows the Kabat numbering scheme (12). The capitalized letter in front of the residue designates heavy chain (H) and light chain (L).

[b] Atom involved in interaction.

**Table S3.** Van der Waals interactions between E2 peptide and AP33 Fab 2[a]

| Fab Residue | Atom[b] | Peptide Residue | Atom[b] | Distance |
|---|---|---|---|---|
| $TYR^{H33}$ | Cδ2 | TRP420 | Cη2 | 4.1 |
| $TYR^{H33}$ | Cε1 | ASN415 | Cβ | 4.0 |
| $TYR^{H33}$ | Cε2 | TRP420 | Cη2 | 3.7 |
| $TYR^{H33}$ | Cε2 | TRP420 | Cζ3 | 3.8 |
| $TYR^{H33}$ | Cζ | ASN415 | N | 3.7 |
| $TYR^{H33}$ | Cζ | TRP420 | Cζ3 | 4.0 |
| $TYR^{H33}$ | Oη | ILE414 | Cα | 3.2 |
| $TYR^{H33}$ | Oη | ILE414 | Cβ | 3.4 |
| $TYR^{H33}$ | Oη | ILE414 | C | 3.6 |
| $TYR^{H33}$ | Oη | TRP420 | Cζ3 | 3.9 |
| $TYR^{H33}$ | Oη | ILE414 | Cγ2 | 4.0 |
| $TYR^{H50}$ | Cε1 | ASN415 | Oδ1 | 3.7 |
| $TYR^{H5}$ | Cζ | ASN415 | Oδ1 | 3.7 |
| $TYR^{H5}$ | Oη | ASN415 | O | 3.5 |
| $TYR^{H5}$ | Oη | ASN415 | Cγ | 3.6 |
| $TYR^{H5}$ | Oη | ASN415 | Cβ | 3.6 |
| $TYR^{H5}$ | Oη | ASN415 | C | 3.7 |
| $TYR^{H53}$ | Oη | ILE414 | Cγ2 | 3.4 |
| $TYR^{H53}$ | Oη | ILE414 | Cβ | 3.9 |
| $TYR^{H58}$ | Cγ | GLY418 | N | 3.8 |
| $TYR^{H58}$ | Cδ1 | GLY418 | Cα | 4.1 |
| $TYR^{H58}$ | Cδ2 | ASN417 | C | 3.5 |
| $TYR^{H58}$ | Cδ2 | GLY418 | N | 3.6 |
| $TYR^{H58}$ | Cδ2 | ASN417 | O | 3.7 |
| $TYR^{H58}$ | Cδ2 | ASN417 | Cα | 3.8 |
| $TYR^{H58}$ | Cδ2 | GLY418 | Cα | 4.2 |
| $TYR^{H58}$ | Cε1 | GLY418 | Cα | 3.9 |
| $TYR^{H58}$ | Cε2 | ASN417 | O | 3.5 |
| $TYR^{H58}$ | Cε2 | ASN417 | C | 3.6 |
| $TYR^{H58}$ | Cε2 | GLY418 | N | 3.8 |
| $TYR^{H58}$ | Cε2 | GLY418 | Cα | 3.9 |
| $TYR^{H58}$ | Cζ | GLY418 | Cα | 3.8 |
| $ILE^{H95}$ | Cγ2 | TRP420 | Cζ2 | 4.3 |
| $THR^{H97}$ | Cγ2 | LEU413 | O | 3.8 |
| $TYR^{H100}$ | Cδ1 | TRP420 | Cζ3 | 3.6 |
| $TYR^{H100}$ | Cδ1 | TRP420 | Cη2 | 3.6 |
| $TYR^{H100}$ | Cδ1 | TRP420 | Cε3 | 3.8 |
| $TYR^{H100}$ | Cδ1 | TRP420 | Cζ2 | 3.9 |
| $TYR^{H100}$ | Cδ1 | TRP420 | Cδ2 | 4.0 |
| $TYR^{H100}$ | Cδ1 | TRP420 | Cε2 | 4.1 |
| $TYR^{H100}$ | Cε1 | TRP420 | Cζ3 | 3.7 |
| $TYR^{H100}$ | Cε1 | LEU413 | Cβ | 3.7 |
| $TYR^{H100}$ | Cε1 | TRP420 | Cε3 | 3.9 |
| $TYR^{H100}$ | Cε1 | TRP420 | Cη2 | 4.2 |
| $TYR^{H100}$ | Cζ | LEU413 | Cβ | 4.0 |

| | | | | |
|---|---|---|---|---|
| $TYR^{H100}$ | Oη | GLN412 | Cβ | 3.6 |
| $TYR^{H100}$ | Oη | LEU413 | Cβ | 3.6 |
| $TYR^{H100}$ | Oη | LEU413 | Cα | 3.9 |
| $TYR^{H100}$ | Oη | LEU413 | Cγ | 3.9 |
| $TYR^{H100}$ | Cδ1 | ILE422 | Cγ1 | 4.1 |
| $TYR^{L28}$ | Cδ1 | ILE422 | Cδ1 | 4.1 |
| $TYR^{L28}$ | Cδ2 | TRP420 | O | 3.7 |
| $TYR^{L28}$ | Cε1 | ILE422 | Cγ1 | 3.8 |
| $TYR^{L28}$ | Cε1 | ILE422 | Cδ1 | 3.8 |
| $TYR^{L28}$ | Cε2 | TRP420 | O | 3.3 |
| $TYR^{L28}$ | Cε2 | HIS421 | Cα A | 4.0 |
| $ASN^{L30}$ | Nδ2 | LEU413 | Cδ1 | 3.7 |
| $PHE^{L32}$ | Cδ1 | TRP420 | Cδ1 | 3.6 |
| $PHE^{L32}$ | Cδ1 | TRP420 | Nε1 | 3.8 |
| $PHE^{L32}$ | Cε1 | TRP420 | Cδ1 | 3.4 |
| $PHE^{L32}$ | Cε1 | TRP420 | Cγ | 3.7 |
| $PHE^{L32}$ | Cε1 | TRP420 | Nε1 | 3.8 |
| $PHE^{L32}$ | Cε1 | TRP420 | Cβ | 4.2 |
| $PHE^{L32}$ | Cζ | TRP420 | Cδ1 | 3.8 |
| $PHE^{L32}$ | Cζ | TRP420 | Cβ | 3.9 |
| $PHE^{L32}$ | Cζ | TRP420 | Cγ | 3.9 |
| $PHE^{L32}$ | Cζ | LEU413 | Cδ1 | 4.1 |
| $ASN^{L91}$ | O | TRP420 | Cδ1 | 3.3 |
| $ASN^{L91}$ | O | GLY418 | O | 3.5 |
| $ASN^{L92}$ | Cα | GLY418 | O | 3.5 |
| $ASN^{L92}$ | Cα | TRP420 | Cδ1 | 4.2 |
| $ASN^{L92}$ | C | GLY418 | O | 3.4 |
| $ASN^{L92}$ | O | SER419 | Cα | 3.7 |
| $ASN^{L92}$ | Cβ | TRP420 | Cδ1 | 4.2 |
| $ASN^{L92}$ | Oδ1 | TRP420 | Cδ1 | 3.3 |
| $ASN^{L92}$ | Oδ1 | TRP420 | Cβ | 3.5 |
| $TRP^{L96}$ | Cε2 | GLY418 | O | 3.7 |
| $TRP^{L96}$ | Cε2 | GLY418 | Cα | 4.0 |
| $TRP^{L96}$ | Nε1 | GLY418 | Cα | 3.3 |
| $TRP^{L96}$ | Nε1 | GLY418 | C | 3.6 |
| $TRP^{L96}$ | Cζ2 | ASN415 | Nδ2 | 3.7 |
| $TRP^{L96}$ | Cζ2 | GLY418 | O | 3.7 |
| $TRP^{L96}$ | Cζ2 | ASN415 | Oδ1 | 3.9 |
| $TRP^{L96}$ | Cζ2 | ASN415 | Cγ | 4.0 |
| $TRP^{L96}$ | Cζ2 | GLY418 | Cα | 4.0 |

[a] Interactions determined by CONTACSYM (18, 19). Numbering for the peptide follows the HCV E2 numbering scheme. Fab numbering follows the Kabat numbering scheme(12). The capitalized letter in front of the residue designates heavy chain (H) and light chain (L).

[b] Atom involved in interaction.

**Table S4.** Hydrogen bond interactions between the E2 peptide and AP33 Fab[a]

| Fab 1 | | | | | Fab2 | | | | |
|---|---|---|---|---|---|---|---|---|---|
| **Peptide Residue** | **Atom Type[b]** | **Fab Residue** | **Atom Type[b]** | **Distance (Å)** | **Peptide Residue** | **Atom Type[b]** | **Fab Residue** | **Atom Type[b]** | **Distance (Å)** |
| LEU413 | N | $TYR^{H100}$ | Oη | 2.8 | LEU413 | N | $TYR^{H100}$ | Oη | 3.2 |
| ASN415 | Oδ1 | $TYR^{H50}$ | Oη | 2.3 | ASN415 | Oδ1 | $TYR^{H50}$ | Oη | 2.8 |
| ASN415 | N | $TYR^{H33}$ | Oη | 2.7 | ASN415 | N | $TYR^{H33}$ | Oη | 3.0 |
| TRP420 | Nε1 | $ASN^{L91}$ | O | 2.8 | TRP420 | Nε1 | $ASN^{L91}$ | O | 2.9 |
| TRP420 | N | $ASN^{L92}$ | Oδ1 | 3.1 | TRP420 | N | $ASN^{L92}$ | Oδ1 | 3.2 |
| GLY418 | O | $TRP^{L96}$ | Nε1 | 3.0 | GLY418 | O | $TRP^{L96}$ | Nε1 | 3.0 |

[a] Hydrogen bonds determined by HBPLUS (14). Numbering for the peptide follows the E2 numbering scheme and numbering for the Fab follows the Kabat scheme (12). The capitalized letter in front of the residue designates heavy chain (H) and light chain (L).

[b] Atom involved in interaction.

## REFERENCES


1. **Adams, P. D., P. V. Afonine, G. Bunkoczi, V. B. Chen, I. W. Davis, N. Echols, J. J. Headd, L. W. Hung, G. J. Kapral, R. W. Grosse-Kunstleve, A. J. McCoy, N. W. Moriarty, R. Oeffner, R. J. Read, D. C. Richardson, J. S. Richardson, T. C. Terwilliger, and P. H. Zwart.** 2010. PHENIX: a comprehensive Python-based system for macromolecular structure solution. Acta Crystallogr. D Biol. Crystallogr. **66:**213-221.
2. **Baker, N. A., D. Sept, S. Joseph, M. J. Holst, and J. A. McCammon.** 2001. Electrostatics of nanosystems: application to microtubules and the ribosome. Proc. Natl. Acad. Sci. U.S.A. **98:**10037-10041.
3. **Chen, V. B., W. B. Arendall, 3rd, J. J. Headd, D. A. Keedy, R. M. Immormino, G. J. Kapral, L. W. Murray, J. S. Richardson, and D. C. Richardson.** 2010. MolProbity: all-atom structure validation for macromolecular crystallography. Acta Crystallogr. D Biol. Crystallogr. **66:**12-21.
4. **Connolly, M. L.** 1993. The molecular surface package. J. Mol. Graphics **11:**139-141.
5. **D'Arcy, A., F. Villard, and M. Marsh.** 2007. An automated microseed matrix-screening method for protein crystallization. Acta Crystallogr. D Biol. Crystallogr. **63:**550-554.
6. **Emsley, P., B. Lohkamp, W. G. Scott, and K. Cowtan.** 2010. Features and development of Coot. Acta Crystallogr. D Biol. Crystallogr. **66:**486-501.
7. **Giang, E., M. Dorner, J. C. Prentoe, M. Dreux, M. J. Evans, J. Bukh, C. M. Rice, A. Ploss, D. R. Burton, and M. Law.** 2012. Human broadly neutralizing antibodies to the envelope glycoprotein complex of hepatitis C virus. Proc. Natl. Acad. Sci. U.S.A.
8. **Ireton, G. C., and B. L. Stoddard.** 2004. Microseed matrix screening to improve crystals of yeast cytosine deaminase. Acta Crystallogr. D Biol. Crystallogr. **60:**601-605.
9. **Kong, L., E. Giang, J. B. Robbins, R. L. Stanfield, D. R. Burton, I. A. Wilson, and M. Law.** 2012. Structural basis of hepatitis C virus neutralization by broadly neutralizing antibody HCV1. Proc. Natl. Acad. Sci. U.S.A. **109:**9499-9504.
10. **Law, M., T. Maruyama, J. Lewis, E. Giang, A. W. Tarr, Z. Stamataki, P. Gastaminza, F. V. Chisari, I. M. Jones, R. I. Fox, J. K. Ball, J. A. McKeating, N. M. Kneteman, and D. R. Burton.** 2008. Broadly neutralizing antibodies protect against hepatitis C virus quasispecies challenge. Nat. Med. **14:**25-27.
11. **Lesley, S. A., P. Kuhn, A. Godzik, A. M. Deacon, I. Mathews, A. Kreusch, G. Spraggon, H. E. Klock, D. McMullan, T. Shin, J. Vincent, A. Robb, L. S. Brinen, M. D. Miller, T. M. McPhillips, M. A. Miller, D. Scheibe, J. M. Canaves, C. Guda, L. Jaroszewski, T. L. Selby, M. A. Elsliger, J. Wooley, S. S. Taylor, K. O. Hodgson, I. A. Wilson, P. G. Schultz, and R. C. Stevens.** 2002. Structural genomics of the *Thermotoga maritima* proteome implemented in a high-throughput structure determination pipeline. Proc. Natl. Acad. Sci. U.S.A. **99:**11664-11669.
12. **Martin, A. C.** 1996. Accessing the Kabat antibody sequence database by computer. Proteins **25:**130-133.
13. **McCoy, A. J., R. W. Grosse-Kunstleve, P. D. Adams, M. D. Winn, L. C. Storoni, and R. J. Read.** 2007. Phaser crystallographic software. J. Appl. Crystallogr. **40:**658-674.
14. **McDonald, I. K., and J. M. Thornton.** 1994. Satisfying hydrogen bonding potential in proteins. J. Mol. Biol. **238:**777-793.
15. **Otwinowski, Z., and W. Minor.** 1997. Processing of X-ray diffraction data collected in oscillation mode. Meth. Enzymol. **276A:**307-326.
16. **Owsianka, A., R. F. Clayton, L. D. Loomis-Price, J. A. McKeating, and A. H. Patel.** 2001. Functional analysis of hepatitis C virus E2 glycoproteins and virus-like particles reveals structural dissimilarities between different forms of E2. J. Gen. Virol. **82:**1877-1883.
17. **Santarsiero, B. D., D. T. Yegian, C. C. Lee, G. Spraggon, J. Gu, D. Scheibe, D. C. Uber, E. W. Cornell, R. A. Nordmeyer, W. F. Kolbe, J. Jin, A. L. Jones, J. M. Jaklevic, P. G. Schultz,**

**and R. C. Stevens.** 2002. An approach to rapid protein crystallization using nanodroplets. J. Appl. Crystallogr. **35:**278-281.

18. **Sheriff, S., W. A. Hendrickson, and J. L. Smith.** 1987. Structure of myohemerythrin in the azidomet state at 1.7/1.3 Å resolution. J. Mol. Biol. **197:**273-296.

19. **Sheriff, S., E. W. Silverton, E. A. Padlan, G. H. Cohen, S. J. Smith-Gill, B. C. Finzel, and D. R. Davies.** 1987. Three-dimensional structure of an antibody-antigen complex. Proc. Natl. Acad. Sci. U.S.A. **84:**8075-8079.

20. **Weiss, M. S., and R. Hilgenfeld.** 1997. On the use of the merging R factor as a quality indicator for X-ray data. J. Appl. Crystallogr. **30:**203-205.